Journal of
Composites Science

MDPI

Article

Comprehensive Analysis of Lubricant and Nanofiller Contributions to Surface Roughness Control in Drilling of GFRP Composites

Mohamed Slamani [1,2,*], Jean-François Chatelain [1] and Siwar Jammel [1]

[1] Mechanical Engineering Department, École de Technologie Supérieure, Montreal, QC H3C 1K3, Canada; jean-francois.chatelain@etsmtl.ca (J.-F.C.); siwarjammel5@gmail.com (S.J.)
[2] Engineering Sciences Research Center, Imam Mohammad Ibn Saud Islamic University (IMSIU), Riyadh 11432, Saudi Arabia
* Correspondence: mohamed.slamani@univ-msila.dz

Abstract

This study investigates the influence of hybrid additives and cutting parameters on the surface roughness (R_a) of drilled Glass Fiber Reinforced Polymer (GFRP) composites. Nine composite panels were fabricated with varying concentrations of wax (0%, 1%, 2%) and graphene (0%, 0.25%, 2%). Drilling experiments were conducted on a CNC milling machine using a range of cutting velocities (50–200 m/min) and feeds (0.02–0.08 mm/rev), and the resulting surface roughness was measured using a profilometer. The results demonstrate that cutting velocity is the most dominant parameter, contributing to 69% of the variability in surface roughness, followed by feed (16%). The incorporation of additives, specifically 1 wt% wax and 0.25 wt% graphene, produced a synergistic effect, yielding the lowest average surface roughness (≈2.9 µm) and the most stable machining process. Higher cutting velocities increased roughness due to thermal effects, while increasing feeds improved surface finish by reducing frictional heating. The findings indicate that an optimal combination of moderate additive concentrations and controlled machining parameters can significantly enhance the surface integrity and process repeatability in the drilling of GFRP composites.

Keywords: surface roughness; GFRP composites; graphene additive; wax lubricant; nanofiller; drilling parameters; machining optimization; sustainability

Academic Editor: Francesco Tornabene

Received: 2 December 2025
Revised: 6 January 2026
Accepted: 29 January 2026
Published: 4 February 2026

1. Introduction

Glass fiber–reinforced polymer (GFRP) composites have gained increasing attention in aerospace, automotive, marine, and construction applications due to their high strength-to-weight ratio, corrosion resistance, and design flexibility [1,2]. Achieving high-quality machining, particularly drilling, is essential for their assembly and structural performance, as 60–80% of composite components require precise drilled holes for fastening [3–5]. However, drilling GFRP and CFRP remains challenging due to their heterogeneous, anisotropic structure, which frequently leads to defects such as fiber pull-out, matrix cracking, delamination, thermal degradation, and poor surface finish [6–9].

Surface roughness (R_a) serves as a key indicator of drilled-hole quality, influencing fatigue life, mechanical performance, and adhesive bonding [10]. Prior studies have shown that surface roughness is highly sensitive to cutting parameters, including spindle speed, feed rate, tool geometry, and lubrication [11–13]. High spindle speeds tend to intensify heat

generation, causing matrix softening and deteriorated surface integrity, whereas higher feed rates can shorten tool–workpiece contact time and improve surface finish [14,15]. These observations highlight the complex thermo-mechanical interactions that govern the final surface morphology during composite drilling. Khanna et al. [16] highlighted the need for ecological and energy-efficient manufacturing processes. Glass fiber reinforced polymer (GFRP) is emerging as a substitute for metallic alloys in automotive and aerospace applications. Two sustainable cutting fluid approaches, dry and liquid CO_2 (LCO_2), have been compared in end milling of GFRP. LCO_2 reduces cutting temperature, tool wear, cutting force, surface roughness, and power consumption compared to dry machining.

Beyond machining parameters, the modification of composite matrices with fillers or additives has emerged as an effective strategy for improving machinability and surface finish. Solid lubricants and nanofillers, including graphite, hBN (Hexagonal Boron Nitride), PTFE (Polytetrafluoroethylene), and graphene, have been shown to enhance thermal conductivity, reduce friction, and stabilize chip formation [17,18]. Graphene, in particular, provides exceptional thermal conductivity, mechanical strength, and a two-dimensional structure that promotes reduced cutting temperatures, less fiber–matrix debonding during drilling [19] and substantially reduced thermal variability [20]. Wax-based additives have also been employed to decrease adhesion between the matrix and cutting tool, thereby improving surface quality, although excessive wax content may lead to inhomogeneous dispersion and diminished machining benefits [21].

Despite extensive research on individual additives and machining parameters, limited attention has been given to hybrid filler systems that combine multiple additives to achieve synergistic improvements in surface finish and machining stability. A wax–graphene hybrid system has the potential to reduce tool–workpiece friction while simultaneously enhancing heat dissipation, yet optimal additive concentrations for minimizing roughness and stabilizing drilling performance remain insufficiently investigated. Moreover, few studies have explored hybrid filler systems combining solid lubricants and nanofillers for synergistic improvement in dry drilling of GFRP, and the relative contributions of machining parameters and hybrid additives to surface roughness variability remain unquantified.

Accordingly, this study examines the combined effects of wax and graphene additives, along with cutting velocity and feed rate, on the surface roughness of drilled GFRP composites. Unlike prior studies focusing on single additives or machining parameters alone, this work presents a combined approach using a wax–graphene hybrid system to simultaneously improve lubrication and heat dissipation. Wax and graphene concentrations were varied systematically, and drilling was performed under multiple cutting conditions to evaluate their individual and interactive influences on surface finish. Statistical tools, including ANOVA, boxplots, and contribution charts, were used to assess process variability and determine the most favorable drilling conditions.

The primary contributions of this investigation include:

1. Demonstrating the synergistic effect of wax–graphene hybrid fillers on surface roughness.
2. Identifying additive concentrations capable of reducing both mean Ra and machining variability.
3. Quantifying the individual and interactive contributions of cutting speed, feed rate, wax content, and graphene content to surface roughness variation, providing a clear guideline for optimized dry drilling of GFRP composites.

These findings provide practical guidance for designing GFRP composites and machining strategies that improve surface quality without the need for specialized coatings, advanced cooling systems, or costly tooling, an outcome of particular relevance to aerospace, automotive, and marine manufacturing sectors.

2. Materials and Methods

2.1. Composite Preparation

A set of composite panels was fabricated using a Glass Fiber Reinforced Polymer (GFRP) as the base material. These panels were modified with varying amounts of two additives, graphene and wax, to evaluate their influence on machining performance. The graphene (Graphene Black 0X, Nano-Xplore Inc., Montréal, QC, Canada) and wax (Ceraflour 996, BYK USA Inc., Wallingford, CT, USA) were incorporated into a Marine 820 epoxy resin, Eaton Rapids, MI, USA, which served as the primary binder.

Nine distinct composite formulations were developed by adjusting the concentrations of wax and graphene. The experimental matrix included three levels of wax (0%, 1%, 2%) and three levels of graphene (0%, 0.25%, 2%), resulting in the following combinations (Table 1):

Table 1. Matrix of Wax and Graphene Concentrations for Each Plate.

Group A (0% Wax)	Group B (1% Wax)	Group C (2% Wax)
A1: 0% Graphene	B1: 0% Graphene	C1: 0% Graphene
A2: 0.25% Graphene	B2: 0.25% Graphene	C2: 0.25% Graphene
A3: 2% Graphene	B3: 2% Graphene	C3: 2% Graphene

The selection of graphene concentrations (0%, 0.25%, and 2%) was informed by prior findings indicating that even very low graphene loadings (around 0.1%) can yield significant improvements in tensile strength and modulus while avoiding issues such as agglomeration and matrix degradation [22]. However, as reported by Cui et al. [23], further increasing the graphene content beyond approximately 2 wt % can lead to diminishing or even adverse effects on mechanical performance due to filler agglomeration and interfacial defects. Accordingly, 0.25% was selected to represent a low-to-intermediate regime where property enhancement begins, and 2% as an upper limit that remains below the threshold at which excessive clustering typically occurs.

To achieve a homogeneous dispersion of the additives, a high-shear mixer (Silverson L5M-A, East Longmeadow, MA, USA) was employed. The mixing procedure consisted of six intervals—four of 2 min and two of 3 min, during which the rotational speed was gradually increased from 1500 to 10,000 RPM. This approach promoted uniform distribution of the particles while minimizing agglomeration.

An ice bath was used to control the heat generated during mixing, ensuring that the resin temperature remained below 30 °C, particularly during high-speed mixing stages. Maintaining a lower temperature also reduced the resin's viscosity, facilitating the removal of entrapped air bubbles.

Air evacuation was performed in two stages. Initially, the mixture underwent a one-hour vacuum treatment at 29 inHg immediately after high-shear mixing to eliminate air introduced during the process. After adding the curing agent, a second 15 min vacuum cycle at a milder vacuum was applied to prevent the formation of new bubbles.

The composite panels were produced using a manual hand lay-up method, selected for its simplicity and cost efficiency (Figure 1a). To facilitate easy removal of the cured panels, the mold surface was first coated with a release agent and covered with a non-stick film. Glass fiber fabric layers were then manually positioned, and the prepared resin mixture was evenly applied to each layer. A roller was employed to expel trapped air and ensure full resin penetration, preventing delamination between layers. In total, 16 fabric layers were stacked, with the fiber orientation alternated at $\pm 90^{\circ}$ to achieve balanced mechanical properties.

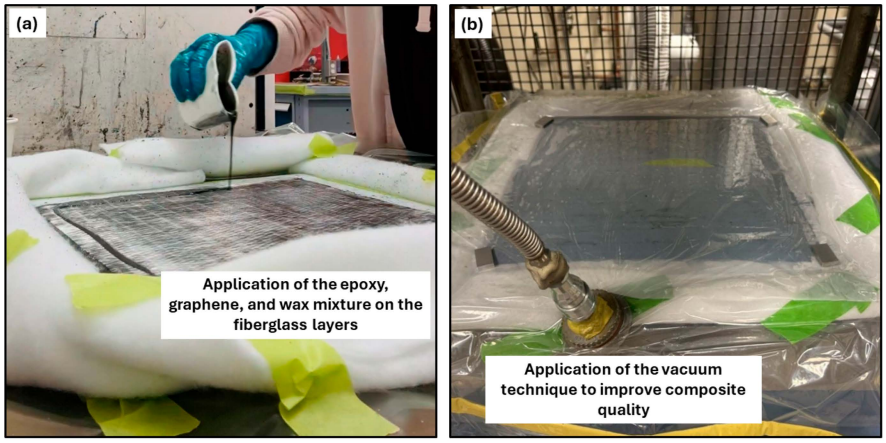

Figure 1. Composite panel fabrication stages: (**a**) lay-up procedure and (**b**) vacuum bag setup.

Once the lay-up was complete, the assembly was enclosed within a vacuum bag to improve fiber compaction and resin distribution (Figure 1b). The laminate was subsequently cured under controlled heat and pressure in a hydraulic press at 60 °C. Spacers of 5 mm thickness were used to maintain uniform panel thickness. The resulting panels, each measuring 12 × 12 in, were prepared for the machining experiments.

2.2. Experimental Setup and Drilling Parameters

The machining analysis was performed on a Huron K2X10 three-axis CNC mill, a high-power unit capable of 28,000 RPM (Figure 2a). To ensure consistency and minimize the influence of tool wear, a new 5.5 mm CVD-coated twist drill (point angle: 118°, helix angle: 30°, two flutes) was used for each composite plate. This approach guaranteed that every drilling condition began with a fresh cutting edge, eliminating wear-induced variability in surface roughness measurements. Additionally, the experimental run order was fully randomized to prevent systematic bias and ensure the statistical validity of the results (Figure 2b). Testing involved four specific cutting settings, where cutting velocities (peripheral speed of the drill) of 50, 100, 150, and 200 m/min corresponding to spindle speeds of approximately 2900, 5800, 8700, and 11,600 rpm, respectively, for a 5.5 mm diameter drill, were systematically matched with feeds of 0.02, 0.04, 0.06, and 0.08 mm/rev, respectively. The cutting velocity and feed pairs were selected based on preliminary tests and industrial practices for GFRP drilling, covering a practical range from conservative to aggressive machining conditions.

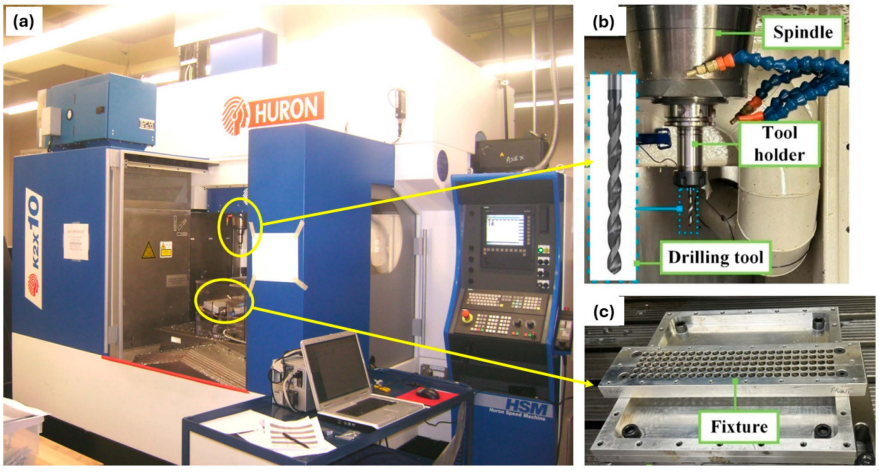

Figure 2. Experimental drilling setup: (**a**) Huron K2X10 three-axis CNC milling machine, (**b**) close-up of the CVD-coated drill bit in operation, (**c**) custom-designed workpiece fixture.

The spindle speed (rpm), feed per revolution (mm/rev), and cutting velocity (m/min) are interrelated machining parameters that together determine the material removal rate and surface quality. The relationship between cutting velocity (V_c), spindle speed (N), and feed per revolution (f) is given by $V_c = f \times N$. This interplay influences heat generation and chip formation, thereby affecting surface roughness. Increasing the spindle speed at a fixed feed reduces the time each cutting edge interacts with the material, which can improve surface finish but may increase thermal loading. Conversely, increasing the feed at a given spindle speed increases material removal per revolution, which can influence surface roughness and tool–workpiece interaction. Understanding these relationships is essential for optimizing drilling conditions and interpreting the statistical contributions of each factor in the regression analysis.

A specialized fixture was built to hold the composite panels firmly in place, ensuring accuracy (Figure 2c). For every material type and speed/feed combination, three holes were drilled to guarantee consistent and statistically significant results.

2.3. Surface Roughness Measurement

Measuring surface roughness on machined FRP (Fiber Reinforced Polymer) components is recognized as a challenging task due to the inherently low repeatability of such measurements. The heterogeneity of the composite material, combined with fiber orientation and local resin distribution, can cause significant variations in roughness readings. To minimize measurement uncertainty and improve reliability, roughness measurements were conducted at five distinct positions around each drilled hole. This multi-point approach ensures a more representative assessment of the surface texture and reduces the influence of localized irregularities.

The surface roughness was evaluated using a Mitutoyo SJ-410 profilometer (Figure 3), following the guidelines of ISO 4284-1997 [24]. The profilometer settings were carefully chosen to capture an accurate representation of the surface topography while remaining consistent across all samples. Table 2 summarizes the key measurement parameters employed during the testing procedure.

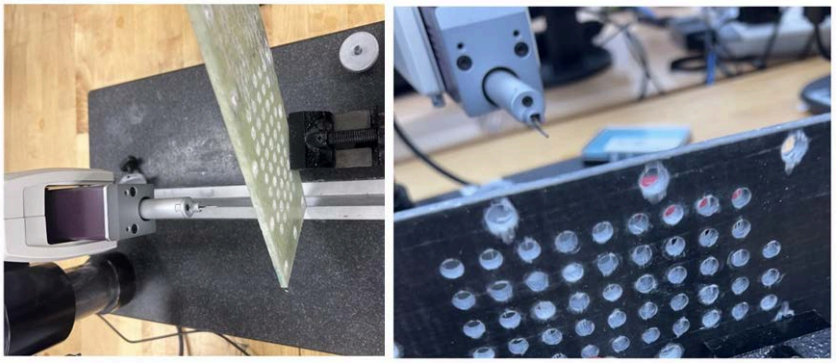

Figure 3. Surface roughness measurement using Mitutoyo SJ-410 profilometer.

Table 2. Profilometer Measurement Parameters.

Parameter	Value
Hole thickness	5 mm
Number of measurements	5
Measurement length	2.5 mm
Evaluation length	12.5 mm
Ra range	2 μm < $R_a \leq$ 10 μm

The procedure ensures that the measured average roughness (R_a) values provide a reliable indicator of the surface quality of the drilled FRP panels. By performing multiple measurements for each hole and maintaining consistent profilometer settings, the experimental uncertainty is minimized, allowing for a more robust analysis of the effects of cutting parameters, material formulations, and additives on surface roughness.

3. Results

The surface roughness (R_a) of the drilled GFRP composites was evaluated under varying cutting parameters and additive compositions. The results are presented through the figures below, highlighting the effects of wax concentration, graphene loading, feed, and cutting velocity, as well as their combined influence on machining performance and process consistency.

3.1. Effect of Cutting Parameters and Reinforcement Additives on Surface Roughness

Figures 4 and 5 provide a detailed analysis of surface roughness (R_a) as a function of cutting conditions, wax concentrations, and graphene concentrations. The dataset includes various cutting velocities (50, 100, 150, and 200 m/min) and feeds (0.02, 0.04, 0.06, and 0.08 mm/rev), as well as different combinations of wax and graphene concentrations. In all error-bar plots, error bars indicate ± 1 standard deviation calculated from three repeated measurements per condition.

Figure 4 shows the effect of feed on surface roughness at different cutting velocities and material compositions. At a cutting velocity of 50 m/min and without wax or graphene, the surface roughness decreases consistently as feed increases from 0.02 mm/rev to 0.08 mm/rev, dropping from 5.784 µm to 2.855 µm. However, at a higher cutting velocity of 200 m/min, the surface roughness becomes more variable, reaching a peak of 9.720 µm at a feed of 0.06 mm/rev, indicating a complex interaction between speed and feed.

Graphene addition at 0.25 wt% significantly improves surface finish compared to the baseline condition. For example, at 50 m/min and 0.02 mm/rev, roughness decreases to 2.419 µm with a relatively low standard deviation (SD = 0.3935 µm), indicating consistent performance.

Figure 5 presents the effect of cutting velocity on surface roughness for varying feeds and material compositions. Higher graphene concentrations (e.g., 2 wt%) do not consistently improve roughness. At 50 m/min and 0.02 mm/rev, a 2 wt% graphene sample results in a roughness of 3.072 µm, higher than the 0.25 wt% graphene condition. This indicates that there is likely an optimal graphene concentration for lubrication and reinforcement effects.

The addition of wax also strongly influences the surface roughness. With 1 wt% wax and 0.25 wt% graphene, one of the lowest roughness values recorded was 1.221 µm at 50 m/min and 0.02 mm/rev. However, the relatively higher standard deviation (0.6483 µm) suggests some variability. Nevertheless, combinations of wax and graphene generally lead to smoother surfaces.

Variability across conditions is evident in the standard deviation results. For example, a standard deviation of 2.094 µm is reported for the baseline (no wax or graphene) at 50 m/min and 0.04 mm/rev. Conversely, with 1 wt% wax and 0 wt% graphene at 150 m/min and 0.08 mm/rev, the standard deviation is much lower (0.1107 µm), indicating greater machining stability.

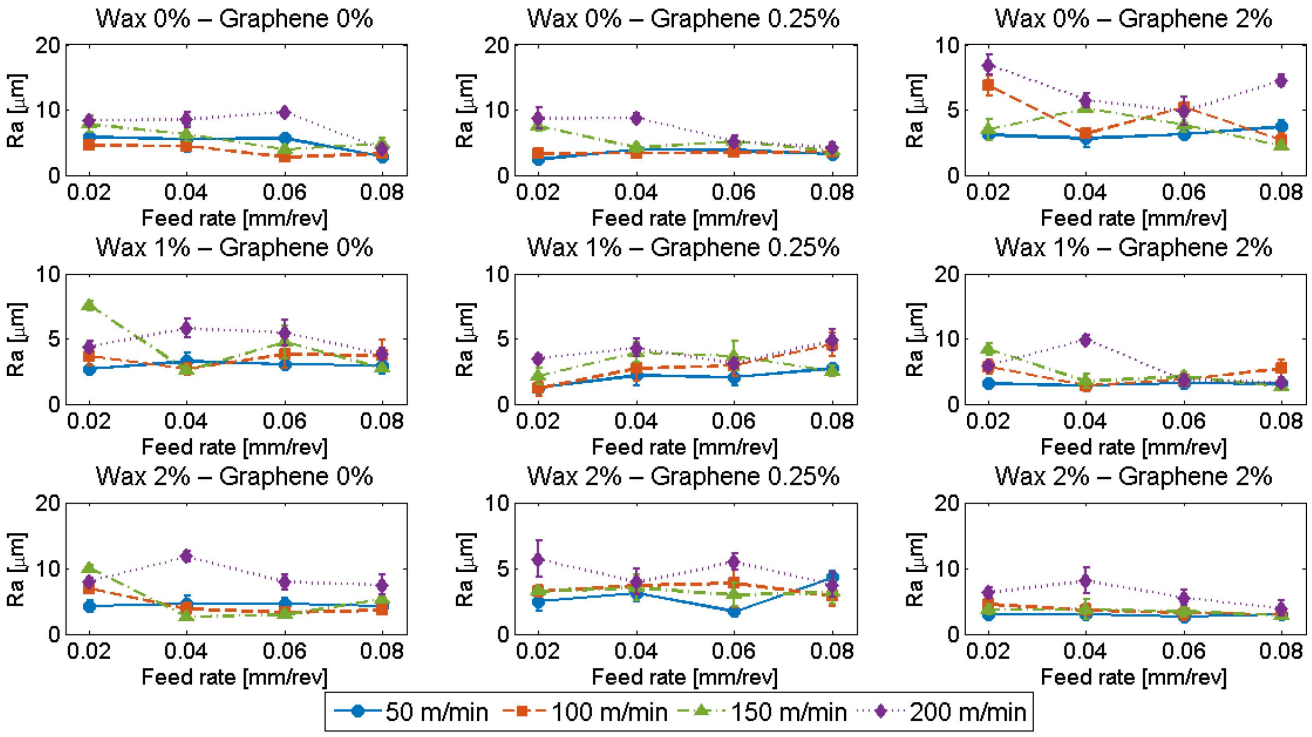

Figure 4. Effect of feed on surface roughness at different cutting velocities and concentrations of wax and graphene.

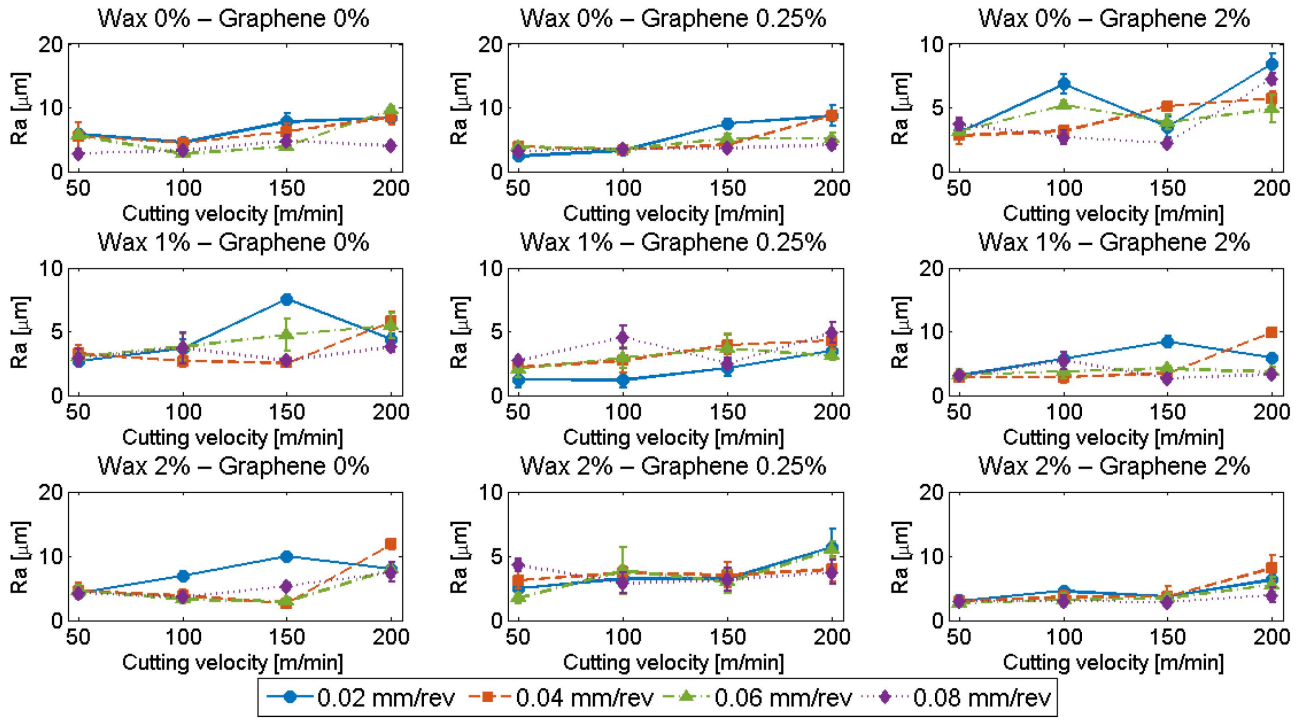

Figure 5. Effect of cutting velocity on roughness at different feeds and concentrations of wax and graphene.

A multiple linear regression model incorporating both main effects and two-factor interactions was developed to investigate the influence of process parameters on the response. The model includes feed rate (f), cutting velocity (V_C), wax (W), graphene (G), and all possible two-factor interactions between these parameters. As shown in Table 3 and illustrated in Figure 6, the regression results indicate that cutting velocity (V_C) is the most

significant factor, explaining approximately 69% of the total variation in the response. The positive coefficient (0.0341) with a low standard error (0.0068) demonstrates a precise and statistically meaningful effect on the response. Feed rate (f) contributes moderately (~16%), although its larger standard error (17.0752) suggests lower precision in the estimate. The other main factors, wax (W) and graphene (G), exhibit relatively minor contributions (2.66% and 0.77%, respectively). Among the interactions, only the feed rate × cutting velocity (f*V) interaction shows a notable contribution of 9.56%, whereas all other interactions contribute less than 1%, implying negligible influence. The intercept (1.6573) represents the baseline response when all factors are at zero.

Table 3. ANOVA table showing regression coefficients, standard errors, F-values, and percentage contributions of main effects and interactions.

Source	Parameter Estimate	Standard Error	F-Value	Percentage	Cumulative %
Intercept	1.6573				
Feed rate (f)	11.6390	17.0752	0.0000	16.0691	16.0691
Cutting velocity (V_C)	0.0341	0.0068	12.8987	69.3914	85.4605
Wax (W)	−0.3652	0.5585	55.7008	2.6587	88.1192
Graphene (G)	0.1456	0.5295	2.1341	0.7726	88.8918
f.V_C	−0.2954	0.1066	0.6202	9.5636	98.4554
f.W	6.2841	7.2984	7.6767	0.9236	99.3790
f.G	−3.2076	6.6975	0.7414	0.2857	99.6647
V_C.W	−0.0012	0.0029	0.2294	0.2064	99.8711
V_C.G	−0.0004	0.0027	0.1657	0.0292	99.9003
W.G	−0.0519	0.1834	0.0234	0.0997	100.0000

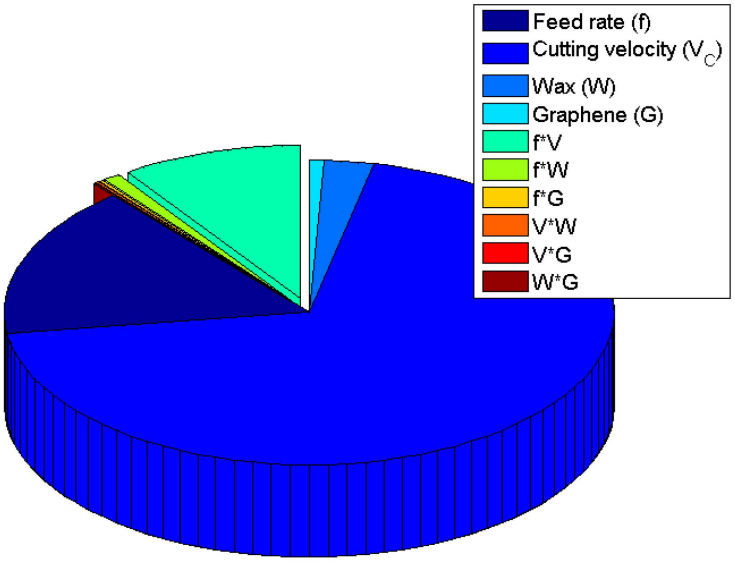

Figure 6. Percentage contribution of main effects and two-factor interactions to the response.

3.2. Effect of Wax Concentration

Figure 7 presents the variation in mean surface roughness with increasing wax concentration (0%, 1%, and 2%). A clear non-linear trend is observed: introducing 1 wt% wax resulted in a significant reduction in surface roughness compared to the unmodified composite, while further increasing the wax content to 2 wt% caused a mild deterioration in surface finish. The lowest average R_a, approximately 3.7 µm, was recorded at 1 wt% wax, compared to 4.8 µm for the wax-free composite. The slight increase at 2 wt% indicates

that excessive wax may lead to unstable lubrication or uneven material flow during cutting. This deterioration at higher concentrations may be attributed to wax particle agglomeration and non-uniform distribution within the matrix, which can disrupt lubrication and heat dissipation. Although direct microstructural evidence (e.g., SEM) was not available in this study, agglomeration at high additive loadings is a well-documented phenomenon in polymer composites [23,24]. These results suggest the existence of an optimum wax concentration that balances lubrication and matrix–fiber cohesion.

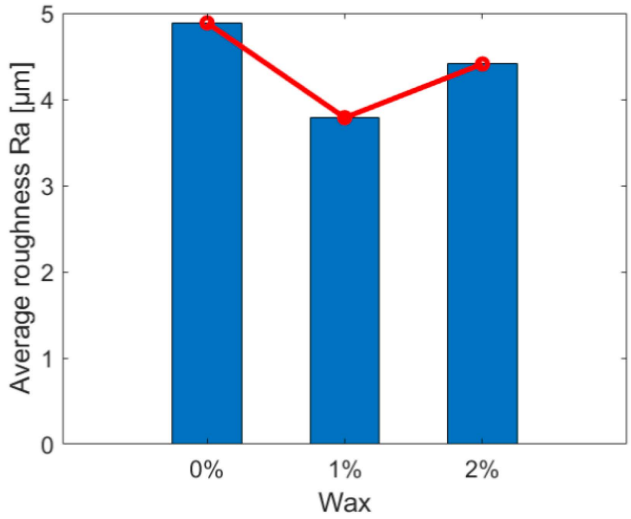

Figure 7. Effect of Wax Concentration on Mean Surface Roughness.

3.3. Effect of Graphene Concentration

The influence of graphene addition on the average surface roughness is depicted in Figure 8. The incorporation of 0.25 wt% graphene significantly improved the surface finish, lowering R_a from about 4.9 µm (0 wt%) to roughly 3.7 µm. However, a further increase to 2 wt% graphene caused a moderate rise in roughness (≈4.3 µm). This performance pattern implies that a small amount of graphene acts effectively as a solid lubricant and thermal conductor, facilitating smooth chip removal and reduced fiber pull-out. Conversely, higher concentrations may induce agglomeration, limiting its uniform distribution within the matrix and disrupting the lubrication efficiency during drilling.

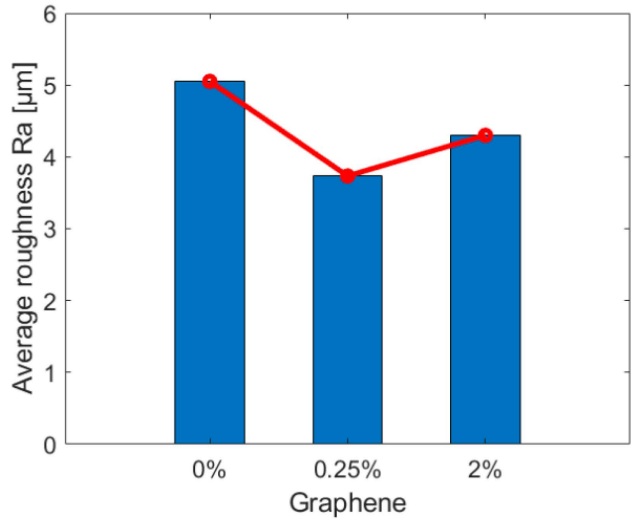

Figure 8. Effect of Graphene Concentration on Mean Surface Roughness.

3.4. Combined Effect of Wax and Graphene

Figure 9 highlights the combined effects of wax and graphene concentrations on surface roughness. The composite containing 1 wt% wax and 0.25 wt% graphene yielded the best overall surface quality, with the lowest average R_a (≈2.9 µm) and the smallest variability—a result superior to those obtained with either additive alone at the same or higher concentrations. This demonstrates a synergistic interaction, where wax reduces adhesive wear while graphene improves heat dissipation, collectively stabilizing the machining process.

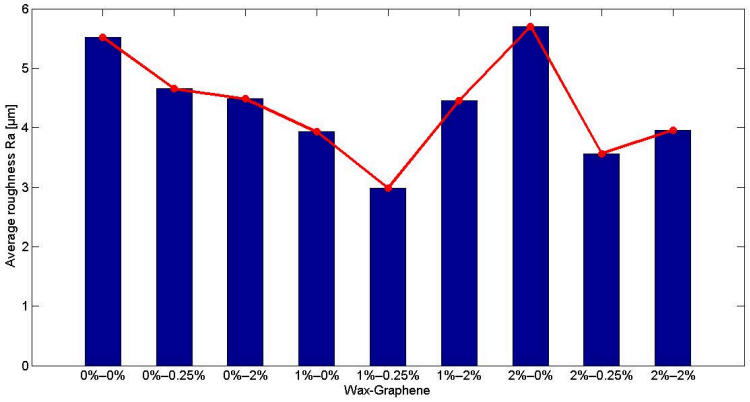

Figure 9. Combined Effect of Wax and Graphene Concentration on Surface Roughness.

Figure 10 arranges the same results in ascending order of roughness, confirming that this hybrid formulation consistently produced the smoothest drilled surfaces across all trials. Increasing both additives beyond their optimal concentrations (2 wt% wax and 2 wt% graphene) slightly increased surface irregularities, likely due to filler clustering and nonuniform tribological behavior.

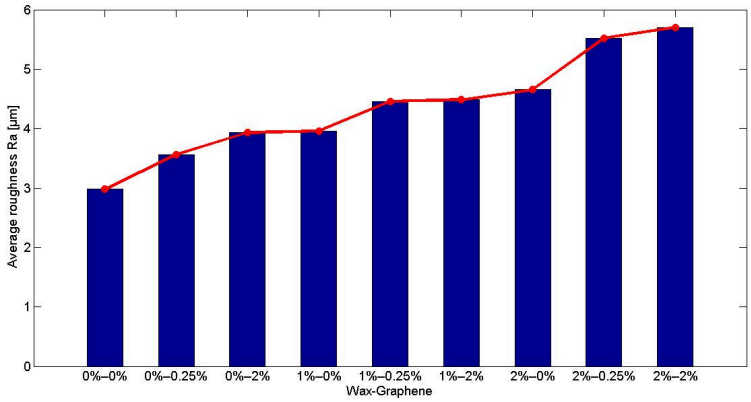

Figure 10. Surface Roughness Values for Different Wax-Graphene Combinations in Ascending Order.

3.5. Effect of Cutting Velocity

Figure 11 shows that the surface roughness increased markedly with cutting velocity. At the lowest cutting velocity of 50 m/min, the mean R_a was approximately 3.6 µm, whereas at 200 m/min it rose to nearly 6 µm. The deterioration in surface quality at higher speeds can be attributed to excessive frictional heat at the tool–workpiece interface, leading to softening of the epoxy matrix and micro-debonding of fibers. Moreover, increased speed accelerates tool wear, causing intermittent fiber tearing and matrix smearing on the drilled surface.

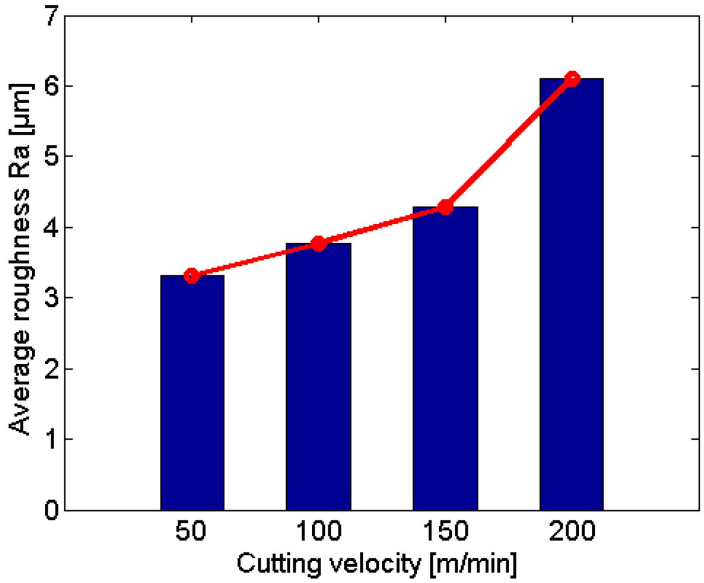

Figure 11. Effect of Cutting Velocity on Mean Surface Roughness.

The spread of roughness values (Figure 12) increased notably at higher speeds, confirming that elevated thermal loads lead to greater variability in surface texture.

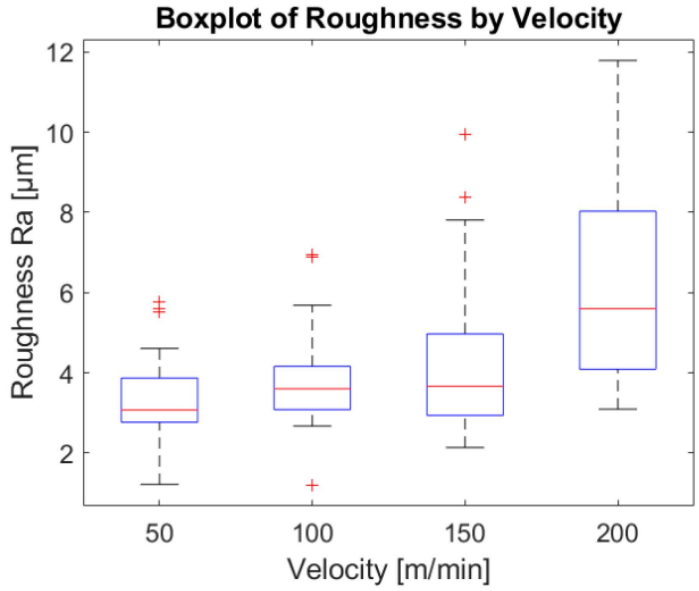

Figure 12. Statistical Distribution of Surface Roughness Across Different Cutting Velocities.

3.6. Effect of Feed

The influence of feed is presented in Figures 13 and 14. The average surface roughness decreased gradually as the feed increased from 0.02 mm/rev to 0.08 mm/rev, with Ra dropping from about 5.0 µm to 3.7 µm (Figure 13). This inverse relationship indicates that higher feeds result in shorter contact time per revolution, thereby reducing frictional heating and preventing excessive matrix softening. The corresponding boxplots in Figure 14 reveal that higher feeds also produced narrower data dispersion, reflecting improved process stability and more uniform surface quality.

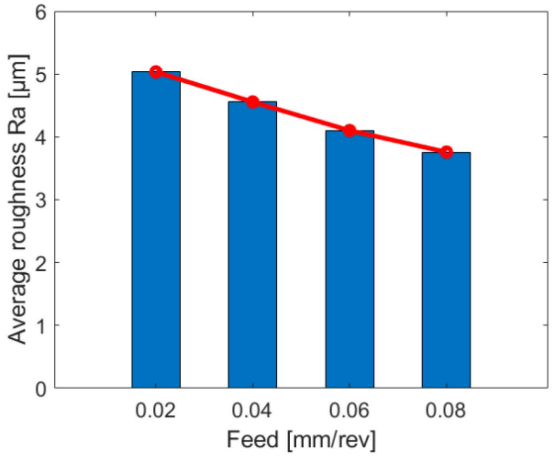

Figure 13. Effect of Feed on Mean Surface Roughness.

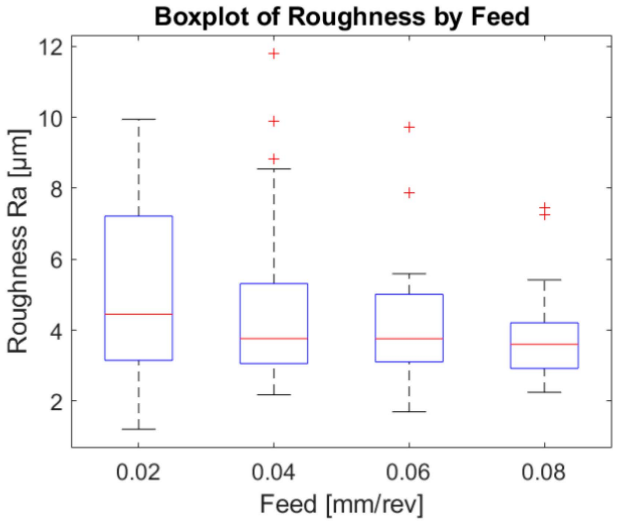

Figure 14. Statistical Distribution of Surface Roughness Across Different Feeds.

3.7. Statistical Distribution of Surface Roughness

The boxplots in Figures 15 and 16 summarize the statistical distributions of surface roughness across different cutting velocities, wax contents, and graphene concentrations.

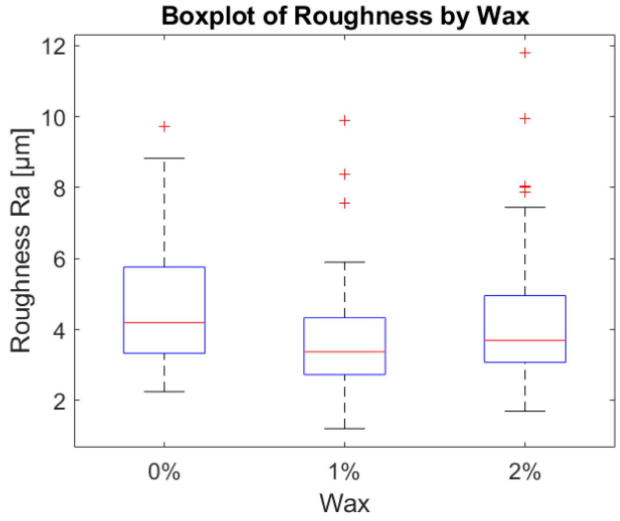

Figure 15. Statistical Distribution of Surface Roughness for Different Wax Concentrations.

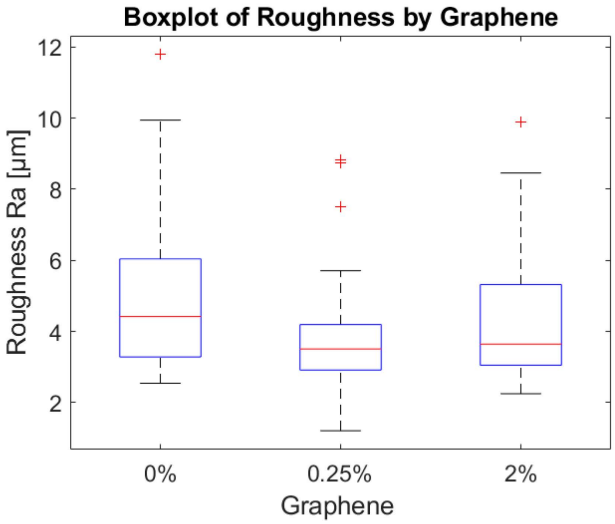

Figure 16. Statistical Distribution of Surface Roughness for Different Graphene Concentrations.

Wax Concentration (Figure 15): The narrowest interquartile range (IQR) was obtained for 1 wt% wax, demonstrating superior reproducibility and machining consistency under optimal lubrication conditions.

Together, these statistical analyses highlight that both moderate additive concentrations and controlled cutting parameters contribute to improved repeatability and surface integrity in GFRP drilling.

3.8. Synthesis of Observations

The overall trends observed above confirm that surface roughness is minimized under low cutting velocities, high feeds, and moderate additive concentrations (1 wt% wax and 0.25 wt% graphene). This condition yields the lowest mean R_a and the least dispersion of results, demonstrating optimal control of thermal and mechanical interactions during drilling. The findings underscore that process stability and surface finish can be simultaneously enhanced through the combined adjustment of machining parameters and hybrid additive formulation.

4. Discussion

The surface roughness of drilled GFRP composites is governed by both machining parameters and additive composition. Moderate amounts of wax and graphene improve surface finish, while excessive concentrations or high cutting velocities degrade it, consistent with known thermo-mechanical mechanisms in composite machining.

4.1. Influence of Additive Composition on Surface Roughness

The lowest surface roughness ($R_a \approx 2.9$ µm) was achieved with 1 wt% wax and 0.25 wt% graphene, representing a ≈40% reduction compared to the unmodified composite, whereas individual additives at the same concentrations yielded only 20–25% reductions. This confirms a synergistic lubricating effect, where wax reduces tool–matrix adhesion [25] and graphene enhances heat dissipation [19,20], collectively minimizing defects such as fiber pull-out and resin smearing.

However, increasing either additive to 2 wt% reversed this improvement, likely due to agglomeration and non-uniform dispersion within the matrix. Such agglomeration disrupts lubrication and chip evacuation, as noted in earlier studies on nanocomposites [21,23,24,26–29].

4.2. Effects of Cutting Velocity and Feed

Surface roughness increased with cutting velocity, from ≈3.6 µm at 50 m/min to ≈6 µm at 200 m/min, due to elevated temperatures that soften the epoxy matrix and promote fiber–matrix debonding [30–32]. In contrast, roughness decreased with increasing feed (0.02–0.08 mm/rev), as shorter tool–workpiece contact limits frictional heating and matrix adhesion [31,33,34].

While direct temperature measurements were not performed in this study, our previous research [20] has shown that graphene addition significantly reduces drilling temperatures in GFRP, supporting the thermal mechanism proposed here.

4.3. Machining Stability and Statistical Repeatability

Boxplot analyses revealed narrow interquartile ranges for the optimal hybrid formulation (1 wt% wax + 0.25 wt% graphene), indicating stable and repeatable machining. Wider variability at higher additive concentrations and cutting speeds reflects unstable thermal and tribological conditions, consistent with findings linking process instability to surface roughness scatter [35].

4.4. Comparative Analysis with Literature Trends

The present findings align with three established trends in composite drilling. First, cutting velocity governs thermal damage and surface degradation [36,37]. Second, feed rate acts as a compensating mechanical factor that reduces heat accumulation and improves surface finish [33,34]. Third, nanofiller and lubricant additives enhance surface integrity by modifying interfacial friction and heat transfer [38]. The observed synergy between wax and graphene further supports the growing literature on hybrid filler systems that simultaneously improve lubrication, heat dissipation, and machining stability [39].

4.5. Mechanistic Interpretation and Industrial Sustainability

Surface quality in GFRP drilling arises from a thermo-mechanical balance: optimal additive concentrations form a stable lubricating film that reduces shear stress, while high speeds promote resin softening and higher feeds reduce thermal exposure. The hybrid wax–graphene system enables high-quality dry drilling with $R_a \approx 2.9$ µm, competitive with lubricated processes.

The optimized dry drilling strategy presented here reduces or eliminates the need for cutting fluids, which are commonly used in GFRP machining to control temperature and improve surface finish. While a direct quantitative comparison with flood cooling or MQL was not performed in this study, the achieved surface roughness (≈2.9 µm) is competitive with values reported in lubricated drilling of similar composites [40,41], suggesting that hybrid additives can enable sustainable dry machining without compromising quality.

By eliminating cutting fluids, this approach also reduces chemical waste, energy consumption for fluid circulation, and post-process cleaning, aligning with green manufacturing objectives and lowering operational costs.

5. Conclusions

This study presents a comprehensive statistical evaluation of surface roughness in drilling GFRP composites using a regression model that explicitly incorporates both main effects and two-factor interaction terms. The inclusion of interaction effects ensures a transparent and statistically sound decomposition of variance and provides a reliable basis for estimating the relative contribution of each factor. To recap, the principal conclusions are as follows.

Cutting velocity remains the most influential parameter, accounting for approximately 69% of the total variation in surface roughness when interactions are included in the model. Its positive coefficient confirms that higher cutting speeds deteriorate surface quality, primarily due to increased thermal loading and epoxy matrix softening. Feed rate contributes about 16%, indicating a secondary but meaningful influence, while the remaining variation is distributed among additives and interaction terms.

The effects of wax and graphene are statistically smaller in isolation; however, their role in process stabilization is evident. The hybrid formulation containing 1 wt% wax and 0.25 wt% graphene consistently produced lower roughness values and reduced variability, confirming a synergistic lubrication effect. At higher concentrations, surface quality deteriorated, likely due to particle agglomeration and non-uniform dispersion, which disrupts effective lubrication and heat evacuation.

Importantly, the interaction analysis demonstrates that surface roughness is not governed solely by individual parameters. The feed–cutting velocity interaction exhibits a measurable contribution to the overall response, confirming that the influence of feed depends on the selected cutting speed. Other interactions contribute marginally but were retained in the model to ensure completeness and to avoid biased attribution of variance.

From an industrial and sustainability perspective, the proposed drilling strategy—combining moderate cutting velocities, relatively higher feeds, and an optimized hybrid additive system—offers a practical route to achieving high surface integrity without reliance on advanced coolants or specialized tool coatings. This approach enhances machining stability, reduces material waste, and supports environmentally responsible manufacturing practices in high-precision sectors such as aerospace and automotive.

6. Limitations and Future Work

This study is limited to a single tool geometry (CVD-coated twist drill), a fixed pairing of cutting velocity and feed levels, and surface roughness evaluation. The potential non-uniform dispersion of additives at high concentrations was not verified via microstructural analysis (e.g., SEM). Future work should expand to include different tool geometries, full factorial parameter sets, direct dispersion characterization, and assessment of additional quality metrics such as delamination, hole cylindricity, and the effect of additives on mechanical properties. Exploration of alternative nanofillers is also recommended for further enhancement of machinability.

Author Contributions: Conceptualization, M.S. and J.-F.C.; methodology, M.S. and S.J.; software, M.S.; validation, M.S. and J.-F.C.; formal analysis, M.S.; investigation, M.S.; resources, J.-F.C.; data curation, S.J.; writing—original draft preparation, M.S.; writing—review and editing, M.S. and J.-F.C.; visualization, M.S.; supervision, J.-F.C.; project administration, J.-F.C.; funding acquisition, J.-F.C. All authors have read and agreed to the published version of the manuscript.

Funding: This research was funded by the Natural Sciences and Engineering Research Council of Canada (NSERC), grant number RGPIN-2017-04305.

Data Availability Statement: Data available upon request.

Acknowledgments: The authors gratefully acknowledge the financial support of the Natural Sciences and Engineering Research Council of Canada (NSERC) under grant #RGPIN-2017-04305.

Conflicts of Interest: The authors declare no conflicts of interest. The funders had no role in the design of the study; in the collection, analyses, or interpretation of data; in the writing of the manuscript; or in the decision to publish the results.

Abbreviations

The following abbreviations are used in this manuscript:

GFRP	Glass Fiber Reinforced Polymer
Ra	Surface Roughness (Arithmetic Average)
SD	Standard Deviation
IQR	Interquartile Range
hBN	Hexagonal Boron Nitride
GFRP	Polytetrafluoroethylene
PTFE	Computer Numerical Control

References

1. Soutis, C. Fibre reinforced composites in aircraft construction. *Prog. Aerosp. Sci.* **2005**, *41*, 143–151. [CrossRef]
2. Slamani, M.; Chatelain, J.-F. A review on the machining of polymer composites reinforced with carbon (CFRP), glass (GFRP), and natural fibers (NFRP). *Discov. Mech. Eng.* **2023**, *2*, 4. [CrossRef]
3. Sheikh-Ahmad, J.Y. *Machining of Polymer Composites*; Springer: Berlin/Heidelberg, Germany, 2009; Volume 387355391.
4. Palanikumar, K. Experimental investigation and optimisation in drilling of GFRP composites. *Measurement* **2011**, *44*, 2138–2148. [CrossRef]
5. Elhadi, A.; Amroune, S.; Slamani, M.; Jawaid, M.; Koklu, U.; Bidi, T. Evaluation of drilling by induced delamination of hybrid biocomposites reinforced with natural fibers: A statistical analysis by RSM. *J. Compos. Mater.* **2024**, *58*, 2515–2530. [CrossRef]
6. Gupta, A.; Vaishya, R.; Kumar, R.; Khan, K.; Chhabra, S.; Verma, A.S.; Bharadwaj, A. Effect of drilling process parameters on delamination factor in drilling of pultruded glass fiber reinforced polymer composite. *Mater. Today Proc.* **2022**, *64*, 1290–1294. [CrossRef]
7. Rajamurugan, T.; Shanmugam, K.; Palanikumar, K. Analysis of delamination in drilling glass fiber reinforced polyester composites. *Mater. Des.* **2013**, *45*, 80–87. [CrossRef]
8. Elhadi, A.; Amroune, S.; Slamani, M. Assessment and analysis of drilling-induced damage in jute/palm date fiber-reinforced polyester hybrid composite. *Biomass Conv. Bioref* **2024**, *15*, 4243–4258. [CrossRef]
9. Urresti-Espilla, I.; Telleria, M.; Llanos, I.; López de Lacalle, L.N. CFRP drilling–induced defect investigation: Part quality characterization and process monitoring approach. *Int. J. Adv. Manuf. Technol.* **2025**, 1–14. [CrossRef]
10. Kumar, D.; Singh, K.; Zitoune, R. Experimental investigation of delamination and surface roughness in the drilling of GFRP composite material with different drills. *Adv. Manuf. Polym. Compos. Sci.* **2016**, *2*, 47–56. [CrossRef]
11. Slamani, M.; Chatelain, J.-F. Kriging versus Bezier and regression methods for modeling and prediction of cutting force and surface roughness during high speed edge trimming of carbon fiber reinforced polymers. *Measurement* **2020**, *152*, 107370. [CrossRef]
12. Slamani, M.; Chatelain, J.-F.; Hamedanianpour, H. Influence of machining parameters on surface quality during high speed edge trimming of carbon fiber reinforced polymers. *Int. J. Mater. Form.* **2019**, *12*, 331–353. [CrossRef]
13. Espilla, I.U.; Telleria, M.; Llanos, I.; de Lacalle, L.N.L. Experimental study on drilling machinability of CFRP: Tool geometry, hole quality and process monitoring analysis. *Procedia CIRP* **2025**, *131*, 80–85. [CrossRef]
14. Prasad, K.S.; Chaitanya, G. Optimization of process parameters on surface roughness during drilling of GFRP composites using taguchi technique. *Mater. Today Proc.* **2021**, *39*, 1553–1558. [CrossRef]
15. Nguyen-Dinh, N.; Hejjaji, A.; Zitoune, R.; Bouvet, C.; Crouzeix, L. Machining of FRP composites: Surface quality, damage, and material integrity: Critical review and analysis. In *Futuristic Composites: Behavior, Characterization, and Manufacturing*; Springer: Berlin/Heidelberg, Germany, 2018; pp. 1–35.
16. Khanna, N.; Rodríguez, A.; Shah, P.; Pereira, O.; Rubio-Mateos, A.; de Lacalle, L.N.L.; Ostra, T. Comparison of dry and liquid carbon dioxide cutting conditions based on machining performance and life cycle assessment for end milling GFRP. *Int. J. Adv. Manuf. Technol.* **2022**, *122*, 821–833. [CrossRef]
17. Mittal, D.; Singh, D.; Sharma, S.K. Thermal characteristics and tribological performances of solid lubricants: A mini review. In *Advances in Rheology of Materials*; IntechOpen: London, UK, 2023.
18. Chan, J.X.; Wong, J.F.; Petrů, M.; Hassan, A.; Nirmal, U.; Othman, N.; Ilyas, R.A. Effect of nanofillers on tribological properties of polymer nanocomposites: A review on recent development. *Polymers* **2021**, *13*, 2867. [CrossRef]
19. El-Ghaoui, K.; Chatelain, J.-F.; Ouellet-Plamondon, C. Effect of graphene on machinability of glass fiber reinforced polymer (GFRP). *J. Manuf. Mater. Process.* **2019**, *3*, 78. [CrossRef]
20. Slamani, M.; Chatelain, J.-F.; Jammel, S. The effect of lubricant and nanofiller additives on drilling temperature in GFRP composites. *J. Compos. Sci.* **2025**, *9*, 558. [CrossRef]
21. Slamani, M.; Jammel, S.; Chatelain, J.-F. Effects of wax and graphene concentrations on cutting force in drilling GFRP composites: A comprehensive study using a full factorial design of experiments. *J. Compos. Mater.* **2025**, *59*, 00219983251341623. [CrossRef]

22. OECD. *Strategies, Techniques and Sampling Protocols for Determining the Concentrations of Manufactured Nanomaterials in Air at the Workplace*; OECD Publishing: Paris, France, 2017.
23. Reif, J.; Rafiee, J.; Wang, Z.; Song, H.; Yu, Z.-Z.; Koratkar, N. Enhanced mechanical properties of nanocomposites at low graphene content. *ACS Nano* **2009**, *3*, 3884–3890. [CrossRef]
24. Kim, H.; Abdala, A.A.; Macosko, C.W. Graphene/polymer nanocomposites. *Macromolecules* **2010**, *43*, 6515–6530. [CrossRef]
25. Khashaba, U. Drilling of polymer matrix composites: A review. *J. Compos. Mater.* **2013**, *47*, 1817–1832. [CrossRef]
26. Şap, S.; Usca, Ü.A.; Uzun, M.; Kuntoğlu, M.; Salur, E.; Pimenov, D.Y. Investigation of the effects of cooling and lubricating strategies on tribological characteristics in machining of hybrid composites. *Lubricants* **2022**, *10*, 63. [CrossRef]
27. Lim, S.K.; Azmi, W.H.; Jamaludin, A.S.; Yusoff, A.R. Characteristics of hybrid nanolubricants for MQL cooling lubrication machining application. *Lubricants* **2022**, *10*, 350. [CrossRef]
28. Song, P.; Cao, Z.; Cai, Y.; Zhao, L.; Fang, Z.; Fu, S. Fabrication of exfoliated graphene-based polypropylene nanocomposites with enhanced mechanical and thermal properties. *Polymer* **2011**, *52*, 4001–4010. [CrossRef]
29. Huang, T.; Zeng, X.; Yao, Y.; Sun, R.; Meng, F.; Xu, J.; Wong, C. Boron nitride@ graphene oxide hybrids for epoxy composites with enhanced thermal conductivity. *RSC Adv.* **2016**, *6*, 35847–35854. [CrossRef]
30. Díaz-Álvarez, A.; Díaz-Álvarez, J.; Santiuste, C.; Miguélez, M. Experimental and numerical analysis of the influence of drill point angle when drilling biocomposites. *Compos. Struct.* **2019**, *209*, 700–709. [CrossRef]
31. Karnik, S.; Gaitonde, V.; Rubio, J.C.; Correia, A.E.; Abrão, A.; Davim, J.P. Delamination analysis in high speed drilling of carbon fiber reinforced plastics (CFRP) using artificial neural network model. *Mater. Des.* **2008**, *29*, 1768–1776. [CrossRef]
32. Yildiz, Y.; Nalbant, M. A review of cryogenic cooling in machining processes. *Int. J. Mach. Tools Manuf.* **2008**, *48*, 947–964. [CrossRef]
33. Khashaba, U. Delamination in drilling GFR-thermoset composites. In Proceedings of the International Conference on Aerospace Sciences and Aviation Technology, Cairo, Egypt, 13–15 May 2003; The Military Technical College: Cairo, Egypt, 2003.
34. Tsao, C.; Hocheng, H. Evaluation of thrust force and surface roughness in drilling composite material using Taguchi analysis and neural network. *J. Mater. Process. Technol.* **2008**, *203*, 342–348. [CrossRef]
35. Shyha, I.; Soo, S.L.; Aspinwall, D.; Bradley, S.; Perry, R.; Harden, P.; Dawson, S. Hole quality assessment following drilling of metallic-composite stacks. *Int. J. Mach. Tools Manuf.* **2011**, *51*, 569–578. [CrossRef]
36. Koplev, A.; Lystrup, A.; Vorm, T. The cutting process, chips, and cutting forces in machining CFRP. *Composites* **1983**, *14*, 371–376. [CrossRef]
37. Davim, J.P.; Reis, P. Drilling carbon fiber reinforced plastics manufactured by autoclave—Experimental and statistical study. *Mater. Des.* **2003**, *24*, 315–324. [CrossRef]
38. Sarıkaya, M.; Güllü, A. Multi-response optimization of minimum quantity lubrication parameters using Taguchi-based grey relational analysis in turning of difficult-to-cut alloy Haynes 25. *J. Clean. Prod.* **2015**, *91*, 347–357. [CrossRef]
39. Sathees Kumar, S.; Kanagaraj, G. Investigation on mechanical and tribological behaviors of PA6 and graphite-reinforced PA6 polymer composites. *Arab. J. Sci. Eng.* **2016**, *41*, 4347–4357. [CrossRef]
40. Shokrani, A.; Dhokia, V.; Newman, S.T. Environmentally conscious machining of difficult-to-machine materials with regard to cutting fluids. *Int. J. Mach. Tools Manuf.* **2012**, *57*, 83–101. [CrossRef]
41. Pusavec, F.; Kramar, D.; Krajnik, P.; Kopac, J. Transitioning to sustainable production–part II: Evaluation of sustainable machining technologies. *J. Clean. Prod.* **2010**, *18*, 1211–1221. [CrossRef]